

Supplementary information for

**Silicate-CoNi-Carbon triple shell sandwich structured  
composite hollow microspheres with low density, boosted  
microwave absorption and high mechanical strength**

Zhenguo An \*, Jingjie Zhang

*Technical Institute of Physics and Chemistry, Chinese Academy of Sciences, Beijing 100190, China*

---

\* Corresponding author. Tel.: +86 10 82543690; fax: +86 10 82543690.

*Email addresses: zgan@ mail.ipc.ac.cn (Z. An), jjzhang@mail.ipc.ac.cn (J. Zhang).*

Table S1 Structure and physical properties of different samples.

Sample	Shell structure	Magnetization ( $M_s$ ) / $\text{emu} \cdot \text{g}^{-1}$	Coercivity ( $H_c$ ) / Oe	Density / $\text{g} \cdot \text{cm}^{-3}$	Survival ratio <sup>(a)</sup> / %
S0	Silicate single shell	—	—	0.38	85.32
S1	Silicate-CoNi-Carbon triple shell	38.55	158.71	0.69	94.36
S2	Silicate-CoNi double shell with granular CoNi shell	46.54	86.24	0.63	88.17
S3	Silicate-CoNi double shell with uniform CoNi particulate shell	36.95	175.02	0.63	92.75

<sup>(a)</sup> The ratio survived hollow microspheres after isopressing at 30MPa.

Table S2 Comparison of the EMW absorption, density and mechanical strength of recently reported similar hollow spherical absorbents.

Material \ Property	RL <sub>min</sub> (dB) / Thickness (mm)	EAB (GHz) / Thickness (mm)	Density (g/cm <sup>3</sup> )	Mechanical strength	Ref.
Carbon twined by CNT <sup>(a)</sup>	-34.56 / 3.2	3.6 / 2.8	—	—	1
Carbonyl iron	-25.5 / 2.0	3.6 / 2.0	—	—	2
CoNi @ Carbon	-44.8 / 3.2	4.0 / 1.6	—	—	3
Sulfur-doped carbon	-51.83 / 1.82	6.08 / 1.82	—	—	4
ZnFe <sub>2</sub> O <sub>4</sub> @ porous carbon	-51.43 / 4.8	3.52 / 4.8	—	—	5
Fe-Carbon	-37.7 / 3.0	7.5 / 3.0	—	—	6
ZnO/MoS <sub>2</sub>	-35.8 / 2.5	10.24 / 2.5	—	—	7
Carbon	-18.13 / 1.6	5.18 / 1.6	—	—	8
Fe <sub>2</sub> O <sub>3</sub> @ RGO <sup>(b)</sup>	-48.1 / 2.5	5.28 / 2.5	—	—	9
Silicate/Fe-Carbon	-18.7 / 2.0	5.7 / 2.0	0.51	—	10
Silicate/NiP/ Co <sub>2</sub> P <sub>2</sub> O <sub>7</sub>	-33.0 / 5.0	1.5 / 4.0	1.18	—	11
Silicate/Ni	-15.0 / 3.5	0.9 / 3.5	0.87	—	12
Silicate/CoNi/Carbon	-55.4 / 2.7	6.8 / 2.3	0.69	94.36% survival <sup>(c)</sup>	herein

<sup>(a)</sup> Carbon nanotubes (CNT);

<sup>(b)</sup> Reduced graphene oxides (RGO);

<sup>(c)</sup> The survival ratio of the hollow particles after isopressing at 30MPa.

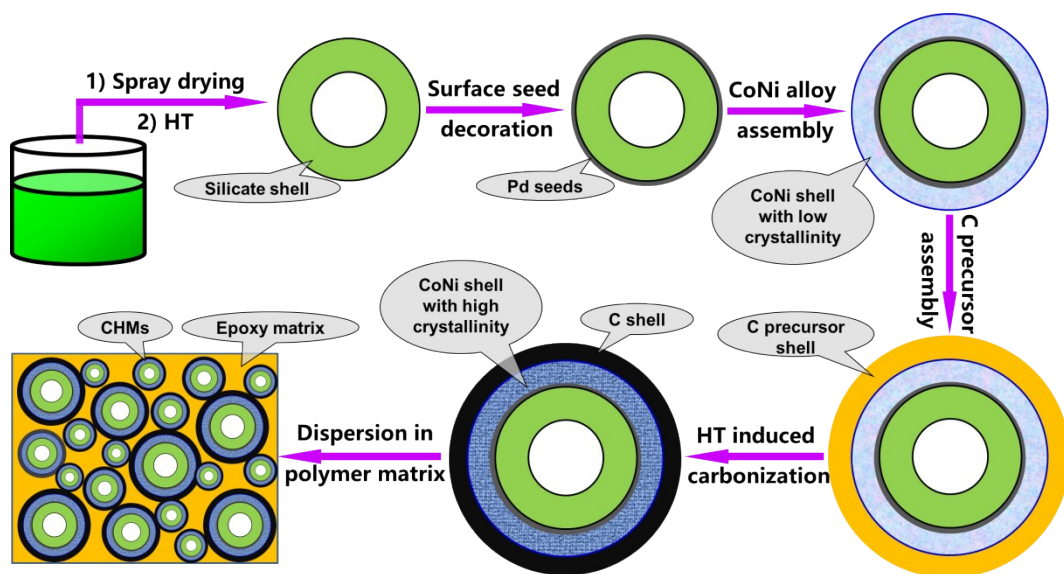


Fig. S1 Schematic illustration of the formation process of the Silicate-CoNi-Carbon triple shell CHMs and their polymer matrix composites.

The hollow microspheres with silicate shell were prepared by spray drying and subsequent high temperature melting process as previously reported. Briefly, an aqueous slurry containing the precursor compounds of the elements that form the silicate shell (Si, O, B, Na, Ca et al) was prepared by mixing and ball-milling of the corresponding raw materials. Then the slurry underwent a spray drying process to form a dry precursor particle with good dispersity. Afterwards, the hollow silicate microspheres were formed through fluidized bed heat treatment of the precursor particles, during which the hollow interior was formed by bubbling of the nitrates and the spherical shape was formed by the driving force of minimizing the surface area of the melted particle and thus the reduced interfacial energy. Afterwards, the CoNi and carbon shell were assembled on the surface of the silicate shell stepwisely through seed induced direct deposition and heattreatment (HT) induced carbonization,

respectively. Finally, the Silicate-CoNi-Carbon triple shell CHMs were dispersed in epoxy matrix to form composites with low density and electromagnetic performances.

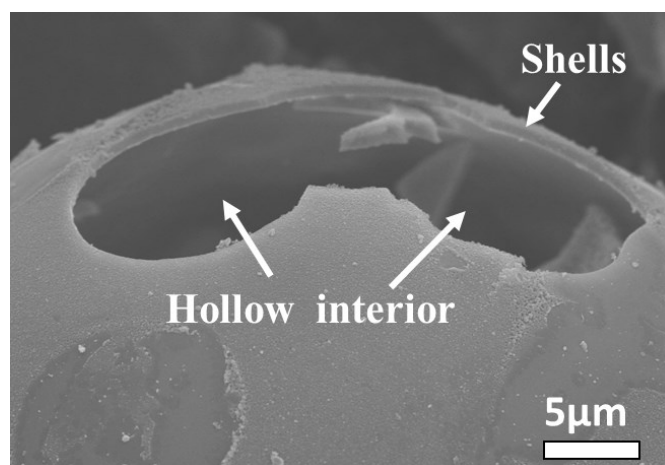


Fig. S2 SEM image of a broken composite hollow microsphere (the white and red arrows point to the hollow interior and the shells, respectively).

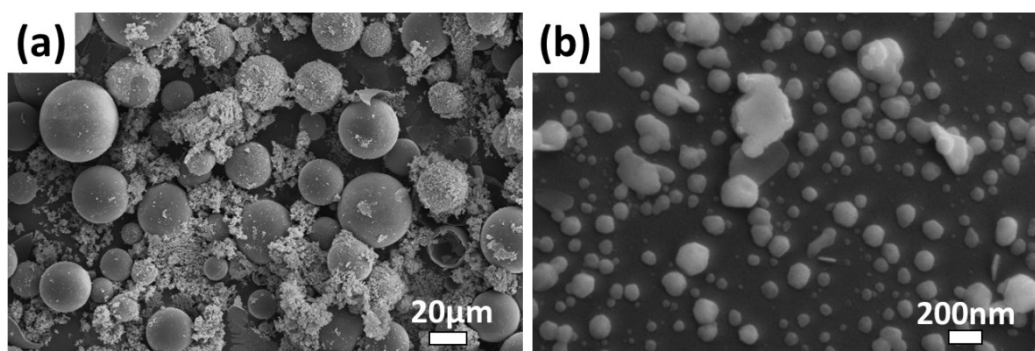


Fig. S3 SEM image of the Silicate-CoNi-carbon precursor composite hollow microspheres prepared via Stöber method: (a) panoramic view and (b) magnified image taken on the surface of a single microsphere.

It has been reported that the Stöber method can also be extended for the preparation of carbon particles and carbon coatings on various supports.<sup>13-16</sup> The polymer

(precursor of carbon) coating on the silicate-CoNi double shell composite hollow microspheres were also carried out according to the literatures for comparison. As can be seen from Fig. S3, the microspheres were not well coated and many isolated phenolic particles were formed, which indicates an inferior coating results. Moreover, the process is relatively time-consuming. We propose the reason lies in that the Stöber method is more suitable to synthesize carbon particles or coatings on nanometer or submicron sizes. In our present case, the silicate-CoNi double shell composite hollow microspheres possess a much bigger size of dozens of micron and a low density of  $0.63 \text{ g}\cdot\text{cm}^{-3}$ . Therefore, the simple mixing-drying process report herein may be more suitable to get relatively thick carbon coatings efficiently on particles with large size. However, since Stöber method is an effective way to prepared carbonaceous materials, with a detailed optimization of the reaction conditions, a better coating result can be expected via an improved Stöber method in the future.

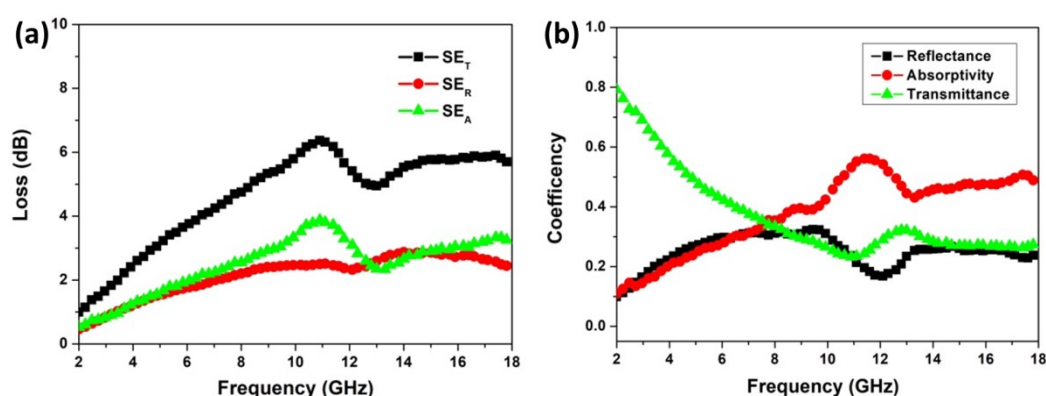


Fig. S4 Frequency dependence of (a) absorbing mechanisms ( $SE_A$  Absorption loss,  $SE_R$  reflection loss and  $SE_T$  total loss) and (b) power balance of sample S1.

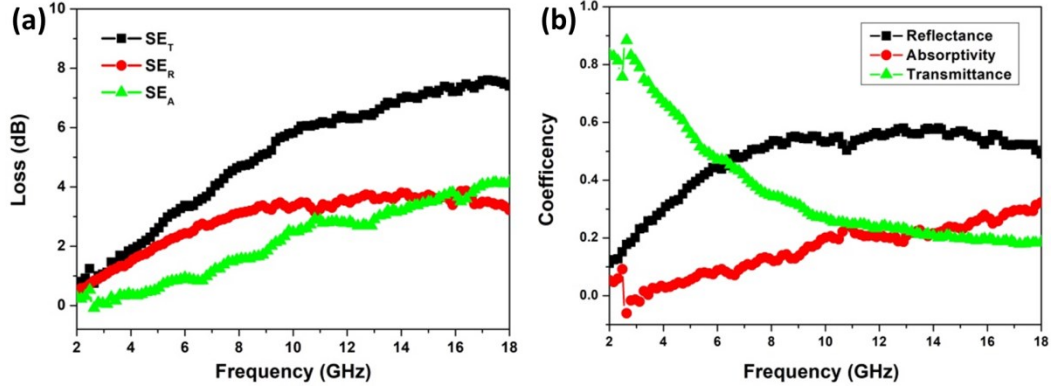


Fig. S5 Frequency dependence of (a) absorbing mechanisms ( $SE_A$  Absorption loss,  $SE_R$  reflection loss and  $SE_T$  total loss) and (b) power balance of sample S2.

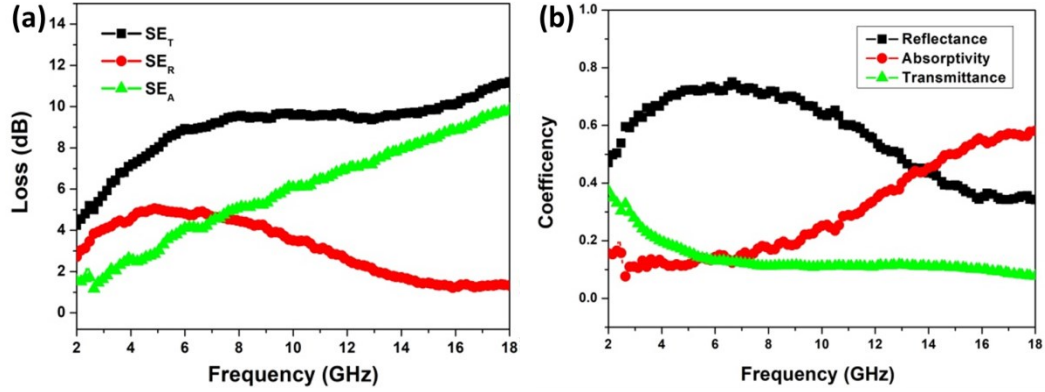


Fig. S6 Frequency dependence of (a) absorbing mechanisms ( $SE_A$  Absorption loss,  $SE_R$  reflection loss and  $SE_T$  total loss) and (b) power balance of sample S3.

The total shielding ( $SE_T$ ), the reflection loss ( $SE_R$ ), the absorption loss ( $SE_A$ ), the reflected (R), transmitted (T) and absorbed (A) parts of the incident EMW powers were calculated using the S parameters:

$$SE_T = SE_R + SE_A \quad (1)$$

$$SE_R = 10 \log_{10} \left( \frac{1}{1 - |S_{11}|^2} \right) \quad (2)$$

$$SE_A = 10 \log_{10} \left( \frac{1 - |S_{11}|^2}{|S_{12}|^2} \right) \quad (3)$$

$$R = |S_{11}|^2 = |S_{22}|^2 \quad (4)$$

$$T = |S_{12}|^2 = |S_{21}|^2 \quad (5)$$

$$A = 1 - R - T \quad (6)$$

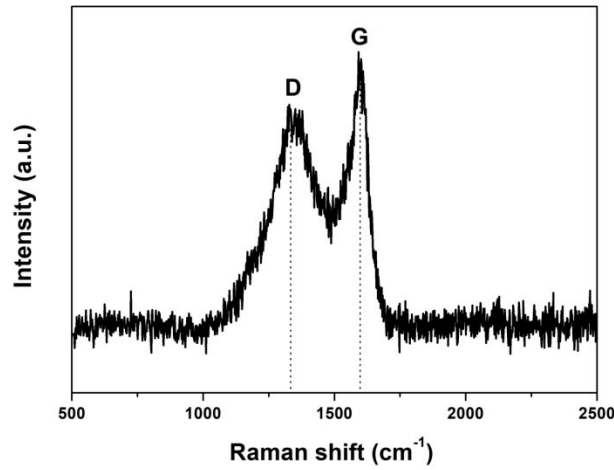


Fig. S7 Raman spectra of the Silicate-CoNi-Carbon triple shell CHMs (S1).

## References

- 1 M. Li, X. Fan, H. Xu, F. Ye, J. Xue, X. Li and L. Cheng, *J. Mater. Sci. Technol.*, 2020, **59**, 164-172.
- 2 M. Jafarian, S. Afghahi, Y. Atassi and M. Salehi, *J. Magn. Magn. Mater.*, 2018, **462**, 153-159.
- 3 Y. Liu, Z. Chen, W. Xie, F. Qiu, Y. Zhang, S. Song, C. Xiong and L. Dong, *J. Alloys Compd.*, 2019, **809**, 151837.



- 4 H. Zhang, Z. Jia, A. Feng, Z. Zhou, C. Zhang, K. Wang, N. Liu and G. Wu, *Compos. Commun.*, 2020, **19**, 42-50.
- 5 L. Chai, Y. Wang, N. Zhou, Y. Du, X. Zeng, S. Zhou, Q. He and G. Wu, *J. Colloid Interf. Sci.*, 2021, **581**, 475-484.
- 6 Z. Deng, Y. Li, H. Zhang, Y. Zhang, J. Luo, L. Liu and Z. Yu, *Compos. Part B*, 2019, **177**, 107346.
- 7 J. Luo, K. Zhang, M. Cheng, M. Gu and X. Sun, *Chem. Eng. J.*, 2020, **380**, 122625.
- 8 J. Tao, J. Zhou, Z. Yao, Z. Jiao, B. Wei, R. Tan and Z. Li, *Carbon*, 2021, **172**, 542-555.
- 9 L. Wang, J. Zhang, M. Wang and R. Che, *J. Mater. Chem. C*, 2019, **7**, 11167-11176.
- 10 Z. An and J. Zhang, *J. Mater. Chem. C*, 2016, **4**, 7979-7988.
- 11 Z. An, J. Zhang and Shunlong Pan, *Dalton T.*, 2010, **39**, 3378-3383.
- 12 Z. An, S. Pan and J. Zhang, *J. Phys. Chem. C*, 2009, **113**, 2715-2721.
- 13 J. Liu, S. Qiao, H. Liu, J. Chen, A. Orpe, D. Zhao and G. Lu, *Angew. Chem. Int. Ed.*, 2011, **50**, 5947-5951.
- 14 A. Fuertes, P. Valle-Vigon and M. Sevilla, *Chem. Commun.*, 2012, **48**, 6124-6126.
- 15 X. Fang, J. Zang, X. Wang, M. Zheng and N. Zheng, *J. Mater. Chem. A*, 2014, **2**, 6191-6197.
- 16 T. Yang, J. Liu, Y. Zheng, M. Monteiro and S. Qiao, *Chem. Eur. J.*, 2013, **19**, 6942-6945.